Next Generation Very Large Array Memo No. 9
Science Working Group 4
Time Domain, Fundamental Physics, and Cosmology

Geoffrey C. Bower[1], Paul Demorest[2], James Braatz[3], Avery Broderick[4], Sarah Burke-Spolaor[2], Bryan Butler[2], Tzu-Ching Chang[5], Laura Chomiuk[6], Jim Cordes[7], Jeremy Darling[8], Jean Eilek[9], Gregg Hallinan[10], Nissim Kanekar[11], Michael Kramer[12], Dan Marrone[13], Walter Max-Moerbeck[2], Brian Metzger[14], Miguel Morales[15], Steve Myers[2], Rachel Osten[16], Frazer Owen[2], Michael Rupen[17], Andrew Siemion[18]

Abstract

We report here on key science topics for the Next Generation Very Large Array in the areas of time domain, fundamental physics, and cosmology. Key science cases considered are pulsars in orbit around the Galactic Center massive black hole, Sagittarius A*, electromagnetic counterparts to gravitational waves, and astrometric cosmology. These areas all have the potential for ground-breaking and transformative discovery. Numerous other topics were discussed during the preparation of this report and some of those discussions are summarized here, as well. There is no doubt that further investigation of the science case will reveal rich and compelling opportunities.

[1]ASIAA, 645 N. A'ohoku Place, Hilo, HI,
[2]NRAO, PO Box O, Socorro, NM,
[3]NRAO, 520 Edgemonet Road, Charlottesville, VA,
[4]Dept. Astronomy, University of Waterloo, Waterloo, ON, Canada
[5]ASIAA, Roosevelt Rd, Taipei, Taiwan

1

[6]Dept. Astronomy, Michgan State Universite, E. Lansing, MI
[7]Dept. Astronomy, Cornell, Ithica, NY
[8]CASA, Univ. Colorado, Boulder, CO
[9]Dept. Physics, New Mexico Tech, Socorro, NM
[10]Dept. Astronomy, Caltech, Pasadena, CA
[11]GMRT, TIFR, Pune, India
[12]MPIfR, auf dem Hügel 69, Bonn, Germany
[13]Dept. Astronomy, Univ. Arizona, Tucson, AZ
[14]Dept. of Physics, Columbia Univ, NY, NY
[15]Dept. Physics, Univ. Washington, Seattle, WA
[16]Space Telescope Science Institute, Baltimore, MD
[17]DRAO, Penticton, BC, Canada
[18]SETI Institute, Mountain View, CA

Contents

1 Introduction

Radio astronomy has played a leading role in the areas of fundamental physics and cosmology. Examples include the discovery of gravitational waves with the binary pulsar, the search for the gravitational wave background with pulsar-timing arrays, the discovery and characterization of the cosmic microwave background, and measurements of black hole properties with very long baseline interferometry. In addition, the time domain has grown from being a small component of radio astronomy to a powerful tool for exploring the Universe. The next generation of radio astronomy instruments, including the Next Generation Very Large Array (ngVLA), have the promise to provide discoveries and measurements with similarly significant impact. The ngVLA entails ten times the effective collecting area of the JVLA and ALMA, operating from 1GHz to 115GHz, with ten times longer baselines (300km) providing mas-resolution, plus a dense core on km-scales for high surface brightness imaging [1].

This report is based on discussions held by the Time-Domain, Cosmology and Physics Scientific Working Group (SWG) in Fall 2014. It also reflects additional material that was presented at the January 2015 AAS Workshop on the ngVLA. The scope of science encompassed by the SWG was quite broad. The committee endeavoured to cover the full breadth in its discussions. An emphasis was made on identifying science cases that were transformational rather than "root-N" improvements on existing cases. Additional emphasis was placed on considering the scientific landscape a decade or more in the future, when ngVLA will come into existence. Numerous topics, many of them worthy of further investigation, were discussed by the SWG but are not presented here for various reasons. These include strong and weak gravitational lensing, pulsar timing, fast radio bursts, active galactic nuclei, cosmic accelerations, the SZ effect, and synoptic surveys. There is no doubt that deeper thought on the scientific case would be valuable.

While many topics were considered of great significance, three topics were considered among the highest impact: Galactic Center pulsar discovery and timing, electromagnetic counterparts to gravitational wave sources, and astrometry. Each of these cases has the potential to lead to transformational discovery.

The technical requirements of the science discussed here is broad. Some cases emphasize the longest ngVLA baselines and/or connections to VLB networks while others are relatively insensitive to angular resolution and predominantly exploit greater sensitivity. Broad frequency coverage was identified as valuable in numerous science cases although there was not a

strict range required. This SWG is probably unique in identification of time domain properties as critical. The science case does not emphasize fast (i.e., sub-second) transients but many classes of slower transients will still require high data rates and real-time processing.

The sections below cover key topics in the areas of time domain, fundamental physics, and cosmology.

2 Time Domain

2.1 Radio Gravitational Wave Countparts

The first direct detection of kHz-frequency gravitational waves (GWs) is anticipated within the next few years once the ground-based interferometers LIGO [2] and VIRGO [3] achieve their planned "advanced" sensitivity. The most promising astrophysical GW sources in the frequency range of these detectors are the inspiral and coalescence of compact object binaries with neutron star (NS) and/or black hole (BH) constituents, which are expected to be detected out to distances of hundreds of Mpc. Although this accomplishment will stand on its own merits, optimizing the science returns from a GW detection will require the identification and study of coincident electromagnetic (EM) counterparts (e.g. [4]). This is important for several reasons, including lifting degeneracies associated with the inferred binary parameters; reducing the minimum signal-to-noise ratio required for a confident GW detection; and identifying the merger redshift, thereby setting the energy scale and allowing an independent measurement of the Hubble constant or other cosmological parameters. The potential wealth of complementary information encoded in the EM signal is likewise essential to fully unraveling the astrophysical context of the event, for example an association with specific stellar populations.

Numerical simulations of the merger of neutron stars with other neutron stars or black holes (e.g. [5]) show that such events typically eject a few hundredths of a solar mass of matter into space with high velocities, $\sim 0.1 - 0.3$ c. This fast ejecta produces a blast wave as it is decelerated by its interaction with the surrounding interstellar medium, powering radio synchrotron emission that could provide a promising GW counterpart [6]. This emission is predicted to peak on a timescale of months to years, at a flux of up to a few tenths of a millijansky at GHz frequencies. The black hole created or newly-fed by the merger is furthermore surrounded by a massisve torus, the subsequent accretion of which may power a transient relativistic jet and a short gamma-ray burst (GRB). The radio afterglow from the GRB

jet may contribute additional bright radio emission. Importantly, unlike the beamed gamma-ray emission, or the beamed optical and X-ray afterglow, the radio emission is expected to be relatively isotropic, making it a more promising counterpart for the majority of GW-detected events. Measuring the radio emission from a NS merger would provide information on the total energy of the ejected matter, its velocity, and the density of the surrounding medium, the latter providing information on whether the merger occured within the host galaxy, or in a lower density medium (e.g. intergalactic space), as would be expected if the binary was given a natal kick at the time of formation of the constituent neutron stars.

One of the biggest uncertainties in predicting the outcome of a NS merger results from our incomplete knowledge of the equation of state (EoS) of high density matter. The recent discovery of massive $\sim 2M_\odot$ neutron stars [7, 8] indicates that the EoS is stiffer than predicted by some previous models. This opens the possibility that some binary neutron star mergers may result in the formation of a long-lived neutron star instead of immediately collapse to a black hole (e.g. [9]). Such a stable remnant is formed rapidly rotating, with a period of $P \sim 1$ ms, and correspondingly large rotational kinetic energy of $E_{\rm rot} \approx 4\pi^2 I/P^2 \approx 3 \times 10^{52}$ erg, where $I \sim 10^{45}$ g cm^2 is the NS moment of inertia. If the merger remnant also possesses a moderately strong dipole magnetic field of $B > 10^{13}$ G, then its electromagnetic dipole spin-down will transfer the rotational energy to the small quantity of ejecta, accelerating it to trans-relativistic speeds, $\Gamma_i \simeq E_{\rm rot}/M_{\rm ej}c^2 > 1$, before the ejecta have been decelerated by the ISM [10]. In this case the radio flux can be orders of magnitude brighter than in the case of black hole formation, with peak fluxes of tens or hundreds of millijanksys for a source at typical distances of LIGO detections. Detecting such events, combined with information on the binary mass available from the gravitational wave signal, could provide stringent constraints on the equation of state of dense nuclear matter.

Discovery and localization of EM GW counterparts will require the ability to survey large areas of sky quickly and sensitively. EM GW signals are expected to be faint, short-lived (days), and localized to a typical accuracy of > 100 deg^2 [11]. Thus, a fast survey capability is required for radio discovery of the EM counterpart. Radio discovery is challenging because of the required survey speed but faces a much simpler identification problem than in the optical, where substantial survey capability will exist but the density of optical transients is very large. Radio observations will play an important role in surveying area as well as following-up on candidates identified through optical or high-energy identification. Higher frequency observations

are critical for energy calorimetry. The very high angular resolution of the ngVLA possibly in coordination with VLBI networks will be powerful for identification of progenitor systems. While Advanced LIGO and VIRGO are turning on in the later part of this decade, uncertain detection rates and source models combined with current capabilities to detect counterparts indicate that ngVLA observations could still play an important role in the discovery and characterization of these sources.

2.2   Jetted Tidal Disruption Events

A rare glimpse into the properties of normally quiescent supermassive black holes (SMBHs) is afforded when a star passes sufficiently close that it is torn apart by the SMBH's tidal gravitational field [12]. Numerical simulations show that the process of disruption leaves a significant fraction of the shredded star gravitationally bound to the SMBH (e.g. Hayasaki et al. 2013). The accretion of this stellar debris has long been predicted to power a thermal flare at optical, UV, and X-ray wavelengths, with over a dozen such thermal flare candidates now identified (e.g. [13] and references therein).

The transient event Swift J1644+57 was characterised by powerful nonthermal X-ray emission [17, 18, 19, 20]. The long duration of Swift J1644+57 and a position coincident with the nucleus of a previously quiescent galaxy led to the conclusion that it was powered by rapid accretion onto the central SMBH following a TDE. The rapid X-ray variability suggested an origin internal to a jet that was relativistically beaming its radiation along our line of sight, similar to the blazar geometry of normal active galactic nuclei [17].

Swift J1644+57 was also characterised by luminous synchrotron radio emission, that brightened gradually over the course of several months [20], as shown in Figure 2.2. Unlike the rapidly varying X-ray emission, the radio emission resulted from the shock interaction between the TDE jet and the dense external gas surrounding the SMBH [21, 17], similar to a GRB afterglow. A second jetted TDE, Swift J2058+05, with similar X-ray and radio properties to Swift J1644+57 was also reported [22].

Jetted TDEs in principle offer a unique opportunity to witness the birth of an AGN, thus providing a natural laboratory to study the physics of jet production across a wide range of mass feeding rates. Obtaining a better understanding of these and future jetted TDEs would thus have far-reaching consequences for topics such as the physics of relativistic jet formation and super Eddington accretion, the conditions (e.g. distribution of accreting or outflowing gas) in nominally quiescent galactic nuclei, and possibly even the astrophysical origin of ultra-high energy cosmic rays [23].
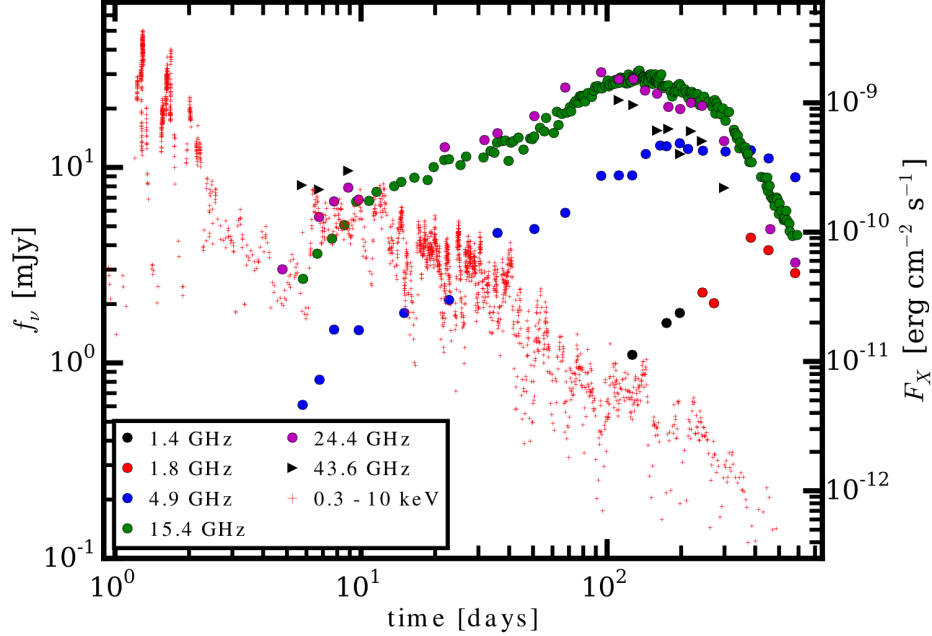
Figure 1: Radio light curves of Swift J1644+57 at observing frequencies 1.4, 1.8, 4.9, 15.4, 24.4 and 43.6 GHz from [14] and [15]. Also shown are the *Swift* XRT observations in the 0.3 − 3 keV band (red crosses, right axis). After several days of peak activity, the X-ray luminosity decreased as a power law $L_x \propto t^{-\alpha}$ in time with $\alpha \sim 5/3$, consistent with the predicted decline in the fall-back rate $\dot{M}$ of the disrupted star [16]. However, the radio emission shows a broad secondary maximum occurring ~ 6 months after trigger, well after the X-ray maximum.

Despite this promise, many open questions remain regarding how jetted TDEs fit into the broader phenomenology of TDEs detected at other wavelengths. It is currently unclear, for instance, what special conditions are required to produce a powerful jet in TDEs. Hydrodynamical models for the evolution of on-axis TDE jets fit to detailed radio light curves can be used to quantify how similar events would appear to observers off the jet axis (e.g. [24]). Such information can be used constrain the presence of off-axis jets in TDEs detected via their quasi-isotropic thermal emission [25, 26] or to assess how jetted TDEs will contribute to future radio transient surveys [21].

Dozens of off-axis ('orphan') TDEs similar to Swift J1644+57 could be discovered by near-term proposed wide-field surveys at GHz frequencies such as Australian Square Kilometer Array Pathfinder and the Very Large Array Sky Survey (VLASS) (e.g. [27]). The low and mid-frequency SKA could detect hundreds of events out to high redshifts $z > 2$ over the course of a 3 year survey. The high sensitivity of the ngVLA would be needed to follow-up and detect these discovered events at high frequencies, helping to confirm their origin as TDEs. The measured redshift distribution of TDEs rate could help constrain the poorly-understood cosmological evolution of low-mass $< 10^8 M_\odot$ SMBHs.

The high frequency radio light curve of Swift J1644+57 is characterized by an unexpected flattening or rebrightening on a timescale of a few months after its initial rise ([14]; Fig. 2.2), with peak fluxes of tens of mJy we obtained at $\sim 10 - 50$ GHz on timescales of a couple hundred days. This behavior contradicted the expectations of simple one-dimensional jet models that assumed energy is added to the blast wave in proportion to the observed X-ray luminosity, and may instead suggest that either the temporal or angular structure of the jet is more complex than commonly assumed (e.g. [14]). Given the relatively slow evolution of TDE radio light curves, the high sensitivity of the ngVLA would allow events like J1644+57 to be monitored for decades or longer. Better characterizing the emission of jetted TDEs at high radio frequencies $\sim 10 - 100$ GHz could be used to constrain the energy scale and angular structure of the jet, as well as to trace the gas density in the parsec-scale environment around previously dormant supermassive black holes.

As the most sensitive contributor to long baseline observations, the ngVLA could also play an important role in resolving TDE jets. The angular size at 30 GHz of a jetted TDE similar to *Swift* J1644+57 near the time of peak radio flux on timescales of a year is expected to be $\ll 0.1$ mas at the distance of this event ($z = 0.354$; [24]). However, for a closer off-axis event at $z = 1$, as could be detected by an upcoming GHz surveys, the jet angular size is predicted to reach > 0.5 mas while its flux still exceeds 1 mJy ([24]; their Fig. 13). Resolving the dual radio lobes from such a source would provide invaluable information on the jet angular structure, such as the possible effects of jet precession due to the black hole spin [28].

3 Fundamental Physics

3.1 Pulsars around Sgr A*

With an average spectral index of -1.7, the flux density spectrum of pulsars is steep. Hence, despite being broadband radio emitters, pulsar observations at high frequencies require a sensitive telescope. The highest frequency that (normal) radio pulsars have been observed at is 134 GHz (Torne et al., in prep.) but the overall sample of mm-observations is currently very limited [29, 30]. But given the decrease in discovered pulsars for smaller galactocentric radii (e.g. [31]) and the overall expectation that interstellar scattering prevents our view [32] to the expected large population of pulsar in the Galactic Center [33], observations at high radio frequencies is exactly what is needed to reveal this previously hidden pulsar population. The ngVLA would be superb instrument to succeed in this task.

The rewards for finding pulsars in the Galactic Center are potentially huge. While high frequency studies of pulsars are also very interesting for providing us with clues for identifying the coherent emission process of pulsars, which still unknown (e.g. [34]), the real motivation is the possibility to study the properties of the central Black Hole (BH) with a exciting level of detail and precision.

Finding pulsars in the Galactic Center. It has been demonstrated that pulsars orbiting Sgr A* will be superb probes for studying the properties of the central supermassive black hole [35, 36, 37]. As shown and discussed further below, it is even sufficient to find and time a normal, slowly rotating pulsar in a reasonable orbit, in order to measure the mass of Sgr A* with a precision of $1 M_\odot(!)$, to test the cosmic censorship conjecture to a precision of about 0.1% and to test the no-hair theorem to a precision of 1%. This is possible even with a rather modest timing precision of $100 \mu s$ due to the large mass of Sgr A* and the measurement of relativistic and classical spin-orbit coupling, including the detection of frame-dragging. Unlike other methods, Liu et al. also developed a method that allows us to test for a possible contamination of the orbital measurements by nearby stars. Given the huge rewards for finding and timing pulsars in the Galactic centre, various efforts have been conducted in the past to survey the inner Galaxy and the Galactic centre in particular (e.g. [38, 39, 40, 41]). None of these efforts has been successful, despite the expectation to find more than 1000 pulsars, including millisecond pulsars (e.g. [33]) or even highly eccentric stellar BH-millisecond pulsar systems [42]. As indicated above, this can be understood in terms of severely increased interstellar scattering due to the highly turbulent medium.

Scattering leads to pulse broadening that cannot be removed by instrumental means and that renders the source undetectable as a pulsar, in particular if the scattering time exceeds a pulse period. The scattering time, however, decreases as a strong function of frequency ($\propto \nu^{-4}$, see e.g. [34]), so that the aforementioned pulsar searches have been conducted at ever increasing frequencies – the latest being conducted at around 20 GHz. The difficulty in finding pulsars at these frequencies is two-fold. We already mentioned that the flux density is significantly reduced due to the steep spectra of pulsars. On the other hand, the reduced dispersion delay, which usually needs to be removed but also acts as a natural discriminator between real pulsar signals and man-made radio interference, is making the verification of a real signal difficult. A phased-up ngVLA that records baseband data would greatly help in both respects. The large sensitivity would allow us to perform deep searches of the Galactic Center. The baseband data can be used to study the frequency structure of the signal in great detail, for instance, by synthesising a very fine polyphase-filterbank or by searching directly for chirped signals.

The serendipitous discovery of the magnetar, PSR J1745-2900, at a separation of 0.1 pc from Sgr A* has led to a new paradigm for understanding Galactic Center scattering and the pulsar population. The pulsar shows much less temporal broadening than predicted based on models for a close scattering screen [43], suggesting that the dominant scattering may occur at much larger distances [44]. In fact, the pulsar was detected at frequencies as low as 1 GHz, where the traditional picture for scattering predicts temporal broadening of 1000 seconds. Secular evolution of the temporal broadening does suggest that some of the scattering may be occuring close to Sgr A*. Reduced temporal broadening, however, does not remove the need for high frequency observations. The scattering predicted for the more distant screen still will lead to timing residuals substantially larger than 100 microseconds for a typical ordinary pulsar and will make millisecond pulsars undetectable at frequencies below 10 GHz. Thus, higher frequency searches and timing will be an important activity for the ngVLA.

Finding pulsars in the Galactic Center will not only lead to unique studies of the general relativistic description of black holes (see below), but we also gain a lot invaluable information about the Galactic Center region itself: the characteristic age distribution of the discovered pulsars will give insight into the star formation history; millisecond pulsars can be used as acceleratormeters to probe the local gravitational potential; the measured dispersion and scattering measures (and their variability) would allow us to probe the distribution, clumpiness and other properties of the central interstellar medium; this includes measurements of the central magnetic field

using Faraday rotation. Figure 1 shows the scattering and dispersion times for different frequencies. One can see that it is even possible to detect millisecond pulsars if the frequency is sufficiently high.

In order to compare the achievable sensitivity to current surveys, we can compare it to the best GBT searches. If we assume that the VLA would have a sensitivity that exceeds that of ALMA significantly, searches at 43 or even 87 GHz would be comparable to those of the GBT around 20 GHz, but with the chance of even detecting millisecond pulsars. At 43 GHz, a significant fraction of the central pulsar population should be detectable, assuming that our currently known population is representative.

Probing the properties of a super-massive BH. As pointed out by [35] and [36], and described in detail by [37], the discovery of radio pulsars in compact orbits around Sgr A* would allow an unprecedented and detailed investigation of the spacetime of this supermassive black hole. As Liu et al. showed, pulsar timing of a single pulsar orbiting Sgr A*, has the potential to provide novel tests of general relativity, in particular confirming the cosmic censorship conjecture and no-hair theorem for rotating black holes. These experiments can be performed by timing observations with 100 μs precision, assuming orbits of S-star-like objects as assumed in the proposal for high-precision optical astrometry observations. It can also be shown (Liu et al 2012, Wex et al. in prep.) that for orbital periods below ~ 0.3 yr, external perturbations can either be ignored or a visibility through parts of their orbits only is sufficient. For full orbits, we expect a $\sim 10^{-3}$ test of the frame dragging and a $\sim 10^{-2}$ test of the no-hair theorem within five years, if Sgr A* is spinning rapidly. The method is also capable of identifying perturbations caused by distributed mass around Sgr A*, thus providing high confidence in these gravity tests. It is worth pointing out that the analysis is not affected by uncertainties in our knowledge of the distance to the Galactic center, R_0 . A combination of pulsar timing with the astrometric results of stellar orbits would greatly improve the measurement precision of R_0.

3.2   Fundamental Constant Evolution

Astronomical spectroscopy in redshifted spectral lines has long been known to provide a probe of changes in the fundamental constants of physics (e.g. the fine structure constant α and the proton-electron mass ratio μ, etc.) over timescales of billions of years. Such temporal evolution is a generic prediction of field theories that attempt to unify the Standard Model of particle physics and general relativity (e.g. [45, 46]). The exciting possibility
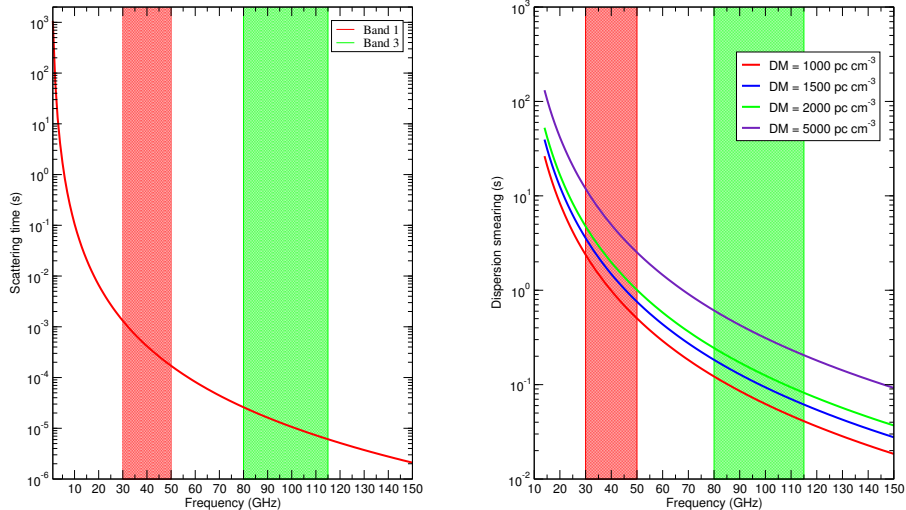
Figure 2: Scattering time (left) and dispersion smearing (right) as a function of observing frequency. Possible observing are indicated in green and red. The scattering time assumes a scattering screen location at 50 pc (see Cordes & Lazio 1997).

of low-energy tests of such unification theories has inspired a number of methods to probe fundamental constant evolution on a range of timescales, ranging from a few years, via laboratory studies, to Gyrs, with geological and astronomical techniques (see [47] for a recent review). Most of these methods, both in the laboratory and at cosmological distances, have been sensitive to changes in the fine structure constant α (e.g. [48, 49, 50, 51]). However, fractional changes in μ are expected to be far larger than those in α in most theoretical scenarios, by factors of $10-500$ (e.g. [52, 53]). In this discussion, we will focus on radio spectroscopic probes of changes in μ over cosmological timescales.

The astronomical methods to probe fundamental constant evolution are typically based on comparisons between the redshifts of spectral lines whose rest frequencies have different dependences on the different constants. These are so far the only approaches that have found statistically significant evidence for changes in *any* constant: Murphy et al. [54, 55] used the many-multiplet method with Keck telescope spectra to obtain $[\Delta\alpha/\alpha] = (-5.4 \pm$

13

$1.2) \times 10^{-6}$ from 143 absorbers with $\langle z \rangle = 1.75$. This result has as yet been neither confirmed nor ruled out (e.g. [56, 57, 51]. More recently, Webb et al. used the many-multiplet method to find tentative evidence of possible spatio-temporal evolution in α, combining results from the Keck-HIRES and VLT-UVES spectrographs [58]. However, these results are all based on optical spectra, where evidence has recently been found for systematic effects in the wavelength calibration, due to distortions in the wavelength scale of echelle spectrographs and the drifts of this scale with time [59, 60, 61].

For many years, ultraviolet ro-vibrational molecular hydrogen (H_2) lines provided the only technique to probe changes in μ on Gyr timescales [62, 63, 64]. The resulting sensitivity to $[\Delta\mu/\mu]$ has been limited by the paucity of redshifted H_2 absorbers (e.g. [65]), the low sensitivity of H_2 lines to changes in μ, and the above systematic effects in wavelength calibration. Despite a number of detailed recent studies, the best limits on fractional changes in μ from this technique are $[\Delta\mu/\mu] \lesssim 10^{-5}$ (2σ) at redshifts $0 < z \lesssim 4$ (e.g. [66, 61, 67]).

The situation has changed dramatically in recent years with the development of new techniques using redshifted radio lines from different molecular species (e.g. [68, 69, 70, 71, 72, 73]). While the number of cosmologically-distant radio molecular absorbers is even smaller than the number of high-z H_2 absorbers – just 5 radio systems [74, 75, 76, 77, 78] – the high sensitivity of tunneling transition frequencies in ammonia (NH_3; [70]) and methanol (CH_3OH; [71, 72]) to changes in μ has resulted in our best present constraints on changes in any fundamental constant on cosmological timescales. For example, Kanekar et al. [79] obtained $[\Delta\mu/\mu] < 2.4 \times 10^{-7}$ (2σ) from a comparison between the redshifts of CS, H_2CO and NH_3 lines from the $z \approx 0.685$ system towards B0218+357, using the Ku-, Ka-, and Q-band receivers of the Green Bank Telescope, while Kanekar et al. ([80]; see also [81, 82]) obtained $[\Delta\mu/\mu] \leq 4 \times 10^{-7}$ (2σ) from CH_3OH lines at $z \approx 0.88582$ towards PKS1830$-$211, using the Ka- and K-band receivers of the Very Large Array (VLA). Note that frequency calibration is not an issue at radio frequencies, with accuracies of ≈ 10 m/s easily attainable even with standard calibration techniques. This is very different from the situation at optical wavelengths where wavelength errors in today's best echelle spectrographs are $\approx 0.5 - 2$ km/s (e.g. [59, 60, 61]).

Radio studies of fundamental constant evolution today are limited by two issues. The first is simply the paucity of redshifted radio molecular absorbers, with only five known systems, all at $z \leq 0.886$. This is likely to change in the near future with the first "blind" surveys for radio molecular absorption at high redshifts [83], currently being carried out with the VLA

and the Australia Telescope Compact Array (ATCA). These surveys should yield samples of molecular absorbers at $z > 1$ that can be followed up in the CH_3OH, NH_3, OH and other lines to probe fundamental constant evolution over large lookback times, ≈ 13 Gyrs. The second issue is simply the raw sensitivity of today's telescopes, at the cm- and mm-wave frequencies of the NH_3 and CH_3OH lines. This limits both the sensitivity of studies of fundamental constant evolution using these spectral lines in systems with detected absorption, as well as the detection of weak spectral lines whose line frequencies have strong dependences on α and μ and hence would yield strong probes of any putative evolution. For example, the Lambda-doubled CH lines (ground state at rest frequencies of ≈ 3.3 GHz) would allow an interesting probe of changes in both α and μ [73]. Similarly, CH_3OH absorption has not so far been detected in the $z = 0.685$ absorber towards B0218+357, and there are multiple CH_3OH lines (e.g. at rest frequencies of ≈ 19 GHz) that have as yet not been detected even in the $z = 0.88582$ system towards PKS1830−211, entirely due to sensitivity issues.

Fig. 3 shows the current state of the art in probes of changes in μ on Gyr timescales; it is clear that results from the NH_3 and CH_3OH techniques are more than an order of magnitude more sensitive than those from H_2 lines. However, the fact that there are only five radio molecular absorbers currently known, and all at $z \leq 0.886$, implies that this high sensitivity is currently only available at $z < 1$, while H_2 lines provide the main technique at higher redshifts. Over the next couple of years, deep spectroscopy with the VLA of the known absorbers towards B0218+357 and PKS1830−211 will allow improvements in the sensitivity to changes in μ by an order of magnitude, to $[\Delta\mu/\mu] \approx few \times 10^{-8}$; these studies are currently under way (e.g. VLA proposal 15A-104). Follow-up VLA and Atacama Large Millimeter Array spectroscopy of new molecular absorbers at $z > 1$ detected in the blind VLA surveys should allow sensitivities of at least $[\Delta\alpha/\alpha] \approx few \times 10^{-7}$. The limitation in sensitivity will then be predominantly from the sensitivity of the VLA, especially since the best NH_3 and CH_3OH transitions for the purpose of probing changes in μ are at cm-wave frequencies, $\approx 12 - 60$ GHz (e.g. [70, 71, 72, 79, 80]).

The proposed ngVLA would thus have a dramatic impact on studies of fundamental constant evolution. The increased sensitivity by an order of magnitude over the VLA would immediately allow an improvement of sensitivity to fractional changes in μ by an order of magnitude, i.e. to $[\Delta\mu/\mu] \approx few \times 10^{-9}$, using the same CH_3OH and NH_3 lines in the two known absorbers towards B0218+357 and PKS1830−211. In addition, the increased sensitivity would allow the detection of multiple CH_3OH lines
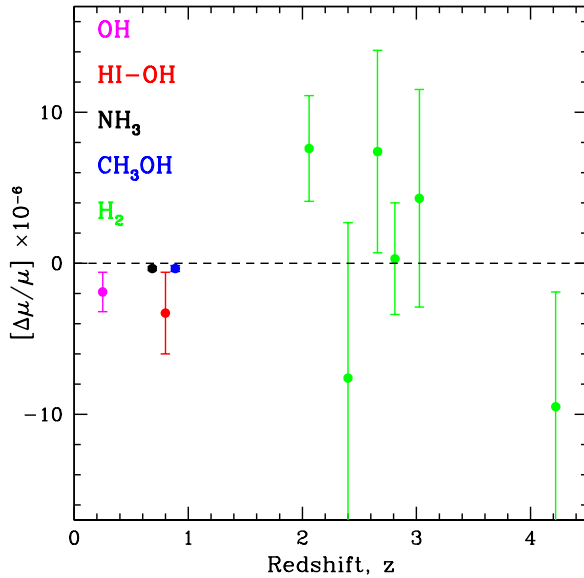
Figure 3: Constraints on changes in μ from various astronomical methods. The four results at $z < 1$ are all from radio techniques, based on comparisons between OH lines [84], OH and HI-21cm lines [85], NH_3 inversion and rotation lines [79], and CH_3OH lines [80], while the six results at $z > 2$ are all based on ultraviolet H_2 lines [86, 66, 87, 61, 88, 67]. It is clear that the radio results from NH_3 and CH_3OH lines are more than an order of magnitude more sensitive than the optical results.

towards B0218+357 as well as the weaker, but more sensitive, CH_3OH lines towards PKS1830−211; these would yield equally sensitive and independent probes of changes in μ in the two absorbers. Similarly, the ngVLA would allow an improvement in sensitivity to $[\Delta\mu/\mu]$ by significantly more than an order of magnitude for the new radio molecular absorbers at $z > 1$, from multiple CH_3OH and NH_3 lines. The ngVLA would also allow the first use of CH lines to probe changes in α and μ, to $z \lesssim 2.3$. It should also allow the detection of multiple transitions from species such as peroxide and methylamine [89, 90], again providing independent probes of changes in μ.

Combining results from different transitions, it should be possible to achieve sensitivities of $[\Delta\mu/\mu] \approx few \times 10^{-10}$ in the two absorbers towards B0218+357 and PKS1830−211, and of $\approx few \times 10^{-9}$ on multiple absorbers at $z > 1$ (which will be identified by the current VLA and ATCA surveys). For comparison, next-generation optical facilities (the TMT and the E-ELT)

should achieve sensitivities of $[\Delta\mu/\mu] \approx 10^{-7}$ with redshifted H_2 lines, over $2 \lesssim z \lesssim 3$. This further assumes that the wavelength calibration problems of current optical echelle spectrographs will be fixed in next-generation spectrographs and that these spectrographs will have high sensitivity in the wavelength range $3000 - 4500$ Å, the wavelengths of the redshifted H_2 lines from absorbers at $z \approx 2 - 3$. It is clear that the ngVLA will have a far higher sensitivity than that of next-generation optical facilities to changes in μ with cosmological time.

The techniques described above are based on absorption spectroscopy of point background sources and hence do not require high angular resolution. High telescope sensitivity is the critical factor in the improvement in sensitivity to fractional changes in μ. A wide frequency coverage is useful, to cover multiple transitions simultaneously. Extending the frequency coverage to ≈ 100 GHz would allow access to high-frequency hydronium transitions [73] at $z \gtrsim 2$, well as interesting transitions from other species (e.g. CH_3NH_2, CH_3OH, etc). Similarly, coverage down to ≈ 1 GHz would allow access to the Lambda-doubled OH lines out to $z \approx 0.7$ as well as the CH lines to $z \leq 2.3$. However, the critical science is based on the cm-wave NH_3 and CH_3OH lines, and hence requires coverage in the frequency range $3 - 50$ GHz, with high spectral resolution and receivers with wide frequency coverage.

3.3 Particle Acceleration and Plasma Physics

It is generally assumed that relativistic particles ("cosmic rays") are energized either in shocks (e.g. supernova remnants) and/or compact objects (e.g. Active Galactic Nuclei). However, the data tell us that particle acceleration also occurs throughout diffuse plasmas (extended radio galaxies, pulsar wind nebulae, the intracluster medium) where shocks either should not occur or cannot produce the necessary electron spectra. Furthermore, the spectra of these objects are not always consistent with predictions of shock acceleration theory.

In addition, we know from plasma physics applied to laboratory and space plasmas that additional particle acceleration mechanisms are possible, and even common. One key process is magnetic reconnection (which occurs when regions of oppositely directed magnetic field are driven together; resistivity in the consequent current sheet dissipates magnetic energy and "reconnects" field lines). Reconnection is known to occur in earth's magnetotail, where it is the source for terrestrial aurora, and also in the sun, where it is the driver for solar flares and Coronal Mass Ejections.

Good spectral information can discriminate between shock and reconnection acceleration. Shock acceleration cannot make particle distributions flatter than E^{-2} [91]; thus the flattest radio spectrum expected from shock acceleration is $\nu^{-0.5}$. By contrast, reconnection acceleration is capable of producing flatter particle distributions (up to E^{-1}; e.g. [92], [93], [94]).

We want to know what is going on in more distant objects – galactic nebulae, extragalactic systems – that accelerates relativistic particles in the extended, diffuse, *filamented* regions we observe? In particular, how important are "local" plasma physics processes (well-understood in space plasmas and the lab) in to more distant astrophysical sources? How much have we been missing by only considering shock acceleration? We choose two examples to illustrate how the ngVLA can answer these questions.
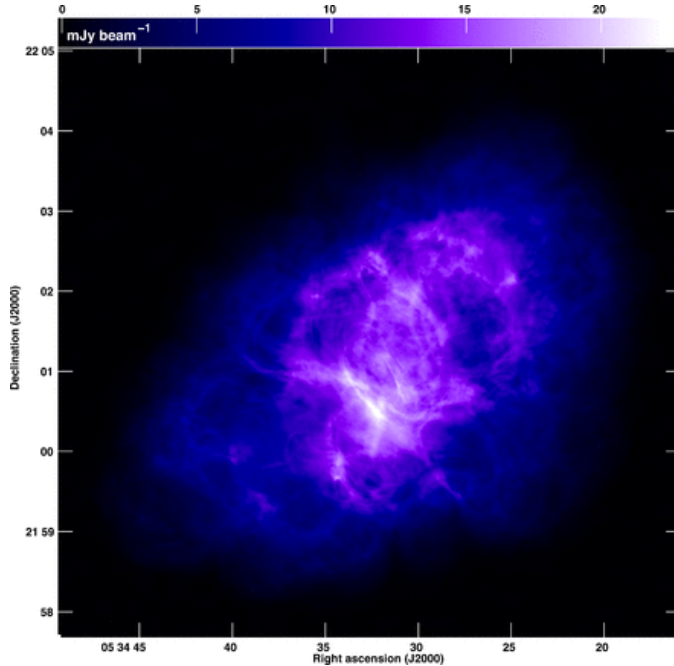
Figure 4: The Crab Nebula at 5 GHz [95]. Current data suggest that extended particle acceleration is happening throughout the Nebula, *by some means other than shock acceleration* – possibly magnetic reconnection. Are the bright filaments the sites of this acceleration? Spatially resolved spectral information, at the highest possible frequencies, from sensitive ngVLA images will test this hypothesis.

Example: the Crab Nebula (Figure 4). Plasma from the pulsar passes through a termination shock and becomes an expanding wind / synchrotron

source which we observe as the Nebula [95]. While many authors have assumed the shock provides the energization needed to make the nebula shine, this can't be the full answer (e.g. [96]). In addition to problems with the likely geometry of the shock [97], the integrated radio spectrum from the Nebula is too flat to be consistent with shock acceleration. Furthermore, while there are some radio spectral gradients across the nebula [98], we do not see a simple gradient away from the shock. Instead, there are flatter spectrum regions throughout the nebula, which suggests distributed acceleration sites; but current observations have neither the resolution nor the frequency sampling to understand the situation. We want to know what creates the distributed acceleration sites throughout the Nebula. Are the synchrotron-bright filaments local shocks in a turbulent wind? Or are they local reconnection sites, or the magnetic flux ropes that are created in a reconnection event? These alternatives can be tested with high-resolution spectral imaging, across the Nebula, to search for small-scale spectral gradients and correlations with radio-bright filaments. High frequencies are needed in order to identify "pristine" reconnection regions (the filaments? elsewhere?), and to learn which process does the accelerating.

Example: the Relic in Abell 2256 (Figure 5). Clusters of galaxies are continually evolving, even at the present epoch, due to ongoing subcluster mergers. Many merging clusters have extended peripheral patches of radio emission (called "relics", [100]). The relics have generally been thought to be shocks driven by the merger (e.g., [101]), and in some cases the data support this theory well (e.g. [102]). Other cases are more challenging, however. Although a large-scale shock has been invoked to explain the relic in Abell 2256 [103], the unusual aspect ratio and strong filamentation of the relic, its high polarization, and the suggestion of very flat radio spectra in the relic's outer reaches [99] are hard to explain with a merger shock. These problems lead one to consider alternative models. Is the relic a gigantic reconnection layer? Are the filaments flux ropes created in the reconnection event (e.g., [104])? Are they field-aligned pinches such as seen in the lab [105] and the terrestrial aurorae ([106]), which provide yet another acceleration mechanism with its own unique spectrum [107]? Once again, discriminating between these models requires broad-band, high-resolution, spectral imaging in order to isolate filament spectra and compare them to the models. Establishing that either reconnection or field-aligned acceleration exists in Abell 2256 will show Mpc-scale, *ordered* magnetic fields exist in the universe.

In order to understand the physics of the objects in question we need good surface brightness imaging, at $\sim$ arcsec resolution, over a wide field (at
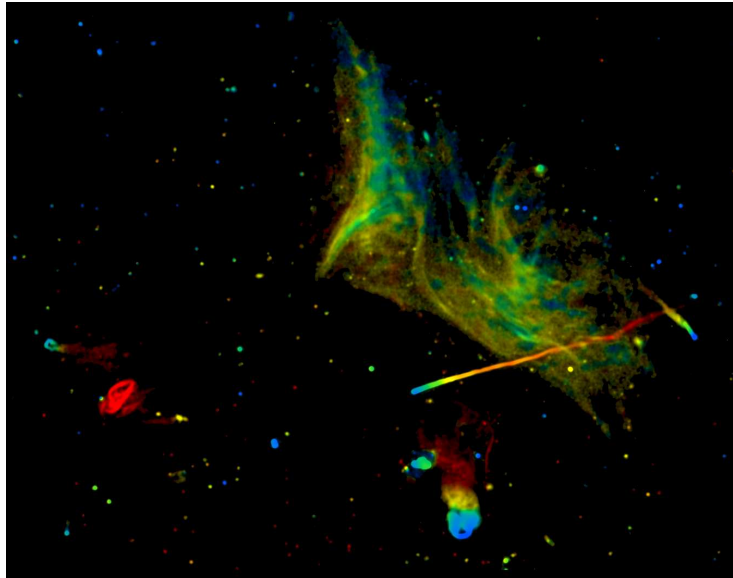
Figure 5:   The galaxy cluster Abell 2256 (z = 0.058) at 1.5 GHz [99]; field of view is 22.′5. This is a "true color" image, shading from dark blue (spectral index $\alpha \lesssim 0.5$) to red (spectral index ≥ 2). The bright, filamented, Mpc-scale structure to the NW is the "cluster relic". We know that in situ particle acceleration is occurring here, but neither the mechanism nor the nature of the bright filaments is understood. Are the filaments post-shock vortices, reconnection sites, or magnetic pinches similar to the earth's aurora? Spatially resolved spectra from ngVLA will be able to discriminate between these models.

least ~ 10 arcmin – presumably with mosaicing), and over a broad frequency range. This is because the critical tests require high-quality, broadband

observations of small features (such as shocks, filaments, flux ropes, on arcsec scales) which exist within a broad, diffuse radio-loud region that can be many arcmin across. We need good surface brightness imaging because the critical features which can discriminate between these models are small and bright, but also embedded in larger, extended emission regions. We need high frequencies because spectra are a key test, and a good spectral sampling across a broad frequency range (at least a decade, ideally more) is needed to measure spectra robustly.

Since the smallest current configuration of the VLA would produce ~ 1 arcsec resolution at 100 GHz, ngVLA must have a very compact configuration with enough collecting area to yield better surface brightness sensitivity than the VLA. Furthermore, the large fields of view required means that ngVLA must work well as a a mosaicing array, since the individual telescopes will have much smaller primary beams than many of the sources of interest (e.g. the Crab Neblua, Abell 2256 and the extended emission in M87 [108], [109]). This requirement also argues for smaller array elements, perhaps 12m, in order to obtain adequate pointing for a mosaic and to reduce the number of pointings needed. Furthermore some total power mode is needed – perhaps like ALMA or using a larger single dish – to sample the largest spatial frequencies. Given the large number of astrophysically interesting sources larger than 30 arcsec, this requirement is likely to be important for many areas of research with ngVLA. For example, the difficult case of A2256 – assuming a compact configuration with 3 times the VLA collecting area, a spectral index of 0.7 and 12m antennas – the relic could be imaged in the 10-50 GHz band using a 400 pointing mosaic with typically 20:1 S/N and 3 arcsec resolution in 25 hours.

3.4 Star-Planet interactions

This working group was tasked with envisioning the astronomical landscape in 10-15 years and then asked to consider the kinds of science questions expected to be topical at that time for which a next generation VLA could provide ground-breaking science. A major effort is underway to find and characterize extrasolar planets, including the environment in which those planets exist: radio observations can play an important role in this effort, through characterization of star-planet interactions. Recent work on star-planet interactions have focussed on "hot Jupiters", expected to have more complex interactions with their host star due to the extreme proximity. These systems are being used as test cases for the kinds of interactions which might be expected from Earth-like planets. It is technologically eas-

ier to find Earth-like planets around low-mass stars (rather than solar-like ones), and these are the types of systems which will be searched for in the nearby universe. Space missions like K2 and TESS, and ground-based searches like the MEarth project all have the goal to find nearby transiting Earth-sized planets so that near-future missions like the James Webb Space Telescope and the next generation of Giant Segmented Mirror Telescopes (E-ELT, TMT, GMT) can perform follow-up characterization of the exoplanet atmosphere. Radio observations provide a unique way to characterize the nature of the accelerated electron population near the star, as well as provide the only method for direct constraints on cool stellar mass loss, important for understanding the radiation and particle environment in which close-in exoplanets are situated.

Star-planet interactions are important tools to learn about the ecology set up by magnetically active stars and their close-in planetary companions. Magnetic reconnection is an inherently non-linear process, motivating observations to make headway, and while there are detailed observations of the Sun, its heliosphere may behave completely differently from that of a magnetically active star with a close-in exoplanet. Stellar radio astronomy excels at constraining the conditions present in outer stellar atmospheres and the stellar near environments: for magnetically active stars, this is typically nonthermal coronal emission [110], although all stars have some amount of mass loss associated with them. Cool stellar mass loss is characterized by an ionized stellar wind, whose radio flux can have a $\nu^{0.6}$ or $\nu^{-0.1}$ dependence if in the optically thick or thin regime, respectively [111, 112]. Mass loss in the cool half of the HR diagram, along/near the main sequence, has been notoriously difficult to detect, due in part to the much lower values of mass loss here compared to other stellar environments (upwards of 10^{-5} solar masses per year for massive stars, compared with 2×10^{-14} solar masses per year for the Sun). Most efforts to detect cool stellar mass loss to date rely on indirect methods; i.e. inferring stellar mass loss by examining absorption signatures of an astrosphere (e.g. [113]). A direct measurement of stellar mass loss through its radio signature would be a significant leap forward not only for understanding the plasma physics of the stars themselves, but also for understanding what kind of environment those stars create. Previous attempts at a direct detection of cool stellar mass loss via radio emission have led to upper limits typically two to three orders of magnitude higher than the Sun's present-day mass loss, while indirect methods find evidence for mass loss rates comparable to or slightly higher than the Sun's present day mass loss rate (up to $\sim$80 times solar $\dot{M}$.) Figure 6 shows the sensitivity to detecting such a feeble ionized stellar wind, for a radio telescope

with the sensitivity of the VLA, and then 5 and 10 times that sensitivity, for a star at 5 and 10 pc. Only for the nearest stars ($\leq$5 pc) and with enhanced, low velocity mass loss are conditions favorable for the present VLA, and enhanced sensitivities are needed to make direct detections over a wider range of stellar parameters. The flat/increasing frequency dependence argues for sensitivity at higher frequencies to probe the transition where this changeover occurs. There are already hints at evaporating planetary atmospheres due to radiation effects of host stars [114], with some evidence for the particle influence of the stellar wind on planetary atmosphere evaporation [115]. These inferences can be tested directly with radio frequency measurements as described above.

Another aspect of star-planet interactions which can be probed with radio observations is the magnetospheric interactions of a magnetized close-in planet with its host star. Similar to the idea that the proximity of two stellar magnetospheres due to close passage can cause periodic episodes of magnetic reconnection (as in [116]), recent results [117] have suggested a triggering mechanism for regularly recurring stellar flares on stars hosting close-in exoplanets (hot Jupiters). To date there have not been any experiments to test this at radio wavelengths, but one can immediately see the advantages of using radio wavelength observations, as the time-dependent response of radio emission reveals the changing nature of the magnetic field strength and number and distribution of accelerated particles. As stellar radio emission typically has a peak frequency near 10 GHz, a wide bandwidth system spanning this range can probe the optically thick and thin conditions, diagnose the changing conditions during the course of a magnetic reconnection flare associated with close passage of an exoplanet, and deduce the nature of the accelerated particle population through measurements of spectral indices from confirmed optically thin emission. This would provide constrains on the accelerated particle population of close-in exoplanets unavailable from any other observational method; such a constraint is necessary to perform detailed modelling of the atmospheres of such exoplanets, due to the influence of accelerated particles in affecting the chemical reactions in terrestrial planet atmospheres [118].

4 Cosmology

4.1 Megamasers

Exquisite observations of the CMB by WMAP and Planck determine the angular-size distance to the surface of last scattering at z $\sim$ 1100, constrain

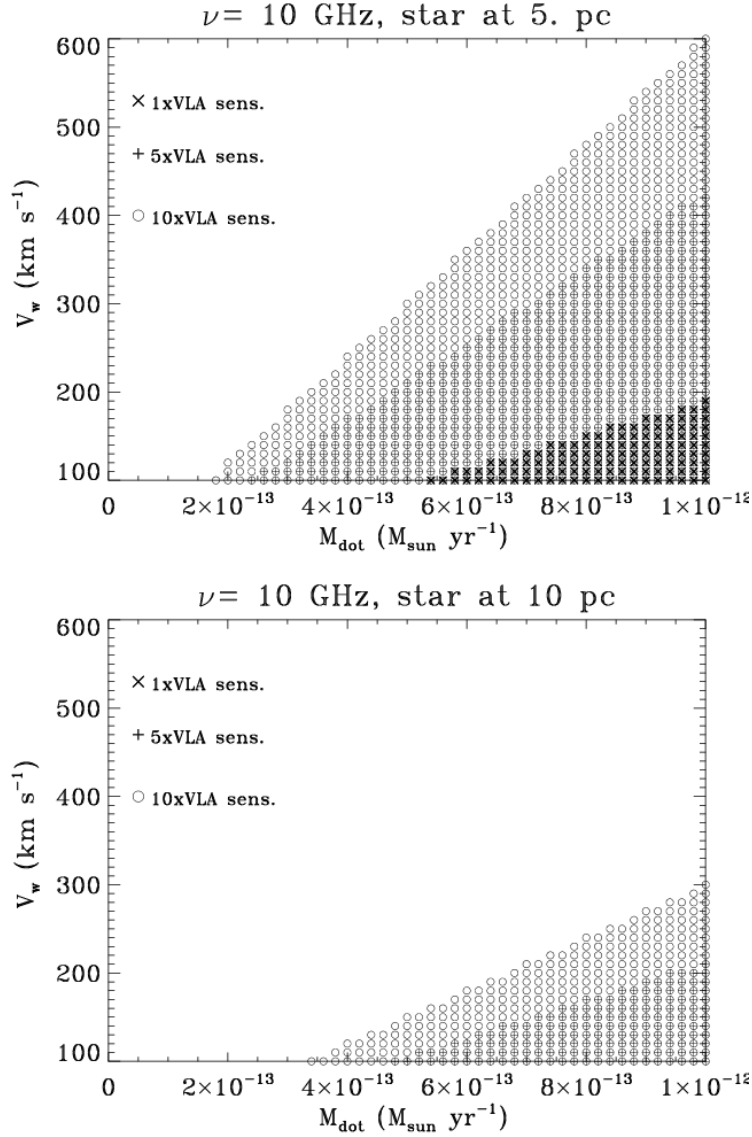Figure 6: Sensitivity to detecting radio emission from an ionized stellar wind, as a function of the wind parameters v_w and $\dot{M}$, for emission at 10 GHz, and assuming the star is at 5 pc **(left)** and 10 pc **(right)**. Three different scenarios are employed: the current VLA sensitivity, scaled up by a factor of 5 (100 nJy rms in 10 hrs) and scaled up by a factor of 10 (50 nJy rms in 10 hrs).

the geometry of the universe to be very nearly flat, and set a basic framework for cosmology. The CMB, however, does not uniquely determine all fundamental cosmological parameters on its own. Observations at z $\sim$ 0, when dark energy is dominant, provide complementary data that constrain critical parameters, including the dark energy equation of state, the geometry of the universe, and the number of families of relativistic particles. CMB observations can *predict* basic cosmological parameters, including H_0, but only in the context of a specific cosmological model. Comparing CMB predictions to astrophysical measurements of H_0 therefore makes a powerful test of cosmological models.

In the context of the standard model of cosmology, i.e. a geometrically flat ΛCDM universe, Planck measurements predict $H_0 = 67.8 \pm 0.9$ km s^{-1} Mpc^{-1} [119]. This result is in tension with recent astrophysical measurements of H_0 based on standard candle observations: $H_0 = 73.8 \pm 2.4$ km s^{-1} Mpc^{-1} [120] and $H_0 = 74.3 \pm 2.6$ km s^{-1} Mpc^{-1} [121]. The implications of this disagreement are of fundamental importance to our understanding of cosmology, so independent measurements of H_0 with unrelated uncertainties are critical to clarify the situation.

Observations of circumnuclear water vapor megamasers in AGN accretion disks can be used to measure direct, geometric distances to their host galaxies, a technique pioneered with observations of NGC 4258 [122]. At only 7.6 Mpc, though, NGC 4258 is too close to measure H_0 directly. However, similar megamasers well into the Hubble flow at D $\sim$ 50 - 200 Mpc are being discovered and studied to measure distances to their host galaxies. With these, the megamaser technique provides H_0 in one step, independent of standard candles and distance ladders.

Over the past decade, astronomers have made an intensive effort to discover and measure H_2O megamasers, spearheaded mainly by the Megamaser Cosmology Project (MCP). Measuring H_0 with this technique requires three types of observations. First is a large survey to identify the rare, edge-on disk megamasers suitable for distance measurments. Second is sensitive spectral monitoring of those disk megamasers to measure secular drifts in maser lines, indicative of the centripetal accelerations of maser clouds as they orbit the central black hole. And third is sensitive VLBI observations to map the maser features and determine the rotation structure and angular size of the disk. The map and acceleration measurements together constrain a model of a warped disk and determine the distance to the host galaxy. The measurement is independent of standard candles and provides H_0 in a single step.

A second important goal in discovering and mapping megamasers is to

measure "gold standard" masses of supermassive black holes (SMBH) by tracing the Keplerian rotation curves of megamaser disks only tenths of a pc from the nuclei and well within the SMBH sphere of influence. About 20 SMBH masses have been measured, to date, using this technique, most with $< 10\%$ uncertainties [123]. These measurements demonstrate a breakdown of the M-σ relation at the low-mass end, implying that any feedback that controls the apparent co-evolution of SMBHs and their elliptical host galaxies has not yet taken hold in spiral galaxies [124]. Larger samples of SMBH mass measurements are required to trace the shape of the M-σ correlation in detail and constrain galaxy and SMBH growth models.
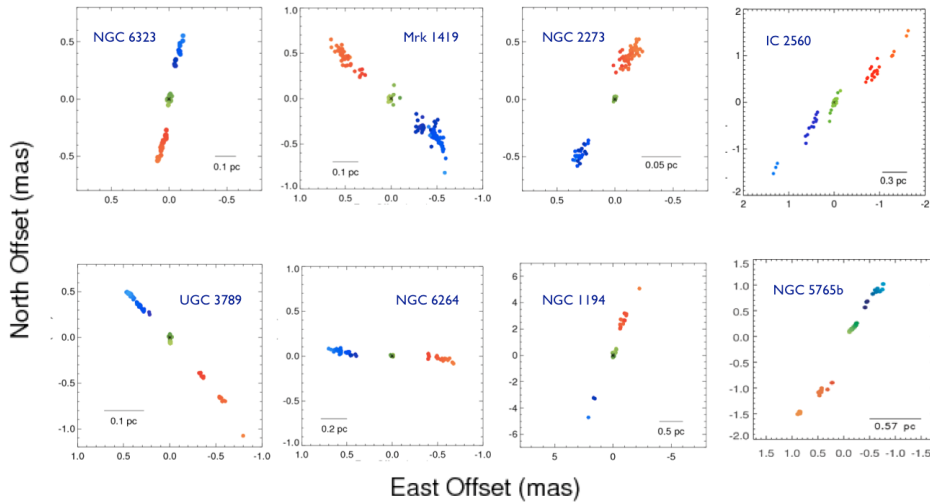
Figure 7: VLBI maps of eight H_2O megamasers showing edge-on disks. These are among the masers currently being studied to measure H_0 directly, using the geometric megamaser technique. Colors represent the line-of-sight velocities of maser clouds. These masers all demonstrate Keplerian rotation.

Of the ~ 30 megamaser systems that have been identified as edge-on disks, ten of them are bright enough and otherwise appropriate for measuring distances. Figure 4.1 shows VLBI maps of eight disk megamasers. Discovering these rare megamasers has required a decade of surveys looking at over 3000 Seyfert 2 galaxies with the GBT. After it is identified as a distance candidate, each megamaser requires a sensitive VLBI map and about two years of monitoring to determine its distance. So far, distances to three have been published: UGC 3789 [125], NGC 6264 [126], and NGC 6323 [127].

Including these published results as well as new work in progress, the mega-maser technique determines $H_0 = 70.4 \pm 3.6$ km s^{-1} Mpc^{-1}, a 5.1% result. This measurement is intermediate between the Planck prediction and the best measurements based on standard candles. In about a year, the MCP will finish measurements and analysis on the remaining disk galaxies, and expects to acheive a $\sim$ 4% measurement. The MCP uses the Green Bank Telescope for surveys and spectral line monitoring, and the High Sensitivity Array (VLBA + GBT + phased VLA + Effelsberg) for VLBI mapping.

The long-term goal of the observational cosmology community is to reach a $\sim$ 1% measurement of H_0 that is robust to the different measurement techniques. To approach a 1% measurement with megamasers, we could measure, for example, $\sim$ 10% distances to each of $\sim$ 100 megamaser galaxies. Such a measurement requires significantly better spectral line sensitivity at 22 GHz than we can achieve with current instruments. In addition, to improve sensitivity of VLBI imaging, approximately 20% of the collecting area should cover long ($\sim$ 5000 km) baselines. Individual maser spots are unresolved, so uv-coverage requirements are modest. For example, the long baselines could be achieved with $\sim$ 5 100-m class apertures. However, long baselines in both the N-S and the E-W directions are important. The recording and correlation capabilities of the new telescope are also modest, but should permit imaging 1 GHz bandwidths contiguously with at least 25 kHz spectral resolution.

4.2   Intensity Mapping

The origin and evolution of structure in the Universe is one of the major challenges of observational astronomy. How and when did the first stars and galaxies form? How does baryonic structure trace the underlying dark matter? A multi-wavelength, multi-tool approach is necessary to provide the complete story or the evolution of structure in the Universe. Intensity mapping is a critical piece of this mosaic. The technique relies on the ability to detect many objects at once through their integrated emission rather than direct detection of individual objects. In particular, this provides a window on lower luminosity objects that cannot be detected individually but that collectively drive important processes.

Intensity mapping experiments that are designed to measure the molecular content of the early universe will provide unique constraints on the history of metal enrichment, interstellar chemistry, galaxy and stellar mass growth, and the structure of the reionization process. This concept fills an otherwise unaddressed gap in our understanding of the growth of galaxies

and complements many major facilities and initiatives of the coming decade. ALMA and EVLA will study the most massive molecular gas reservoirs at $z > 2$, while intensity mapping experiments provide essential context for these rare giants by measuring the emission of the bulk population of galaxies. Similarly, major optical and infrared facilities, including JWST, will reveal the formed stars and ionizing radiation in the EoR, but the natal material that fuels this star formation can only be observed in molecular lines. The radio arrays searching for EoR 21cm emission neutral hydrogen [128, 129, 130] will trace the ionizing bubbles around the galaxies seen with molecular intensity mapping; ultimately, the cross-correlation of the molecular and neutral atomic gas signals will provide a direct view of the growth of ionization bubbles and an important, systematically cleaner, validation of 21cm power spectra [131]. Finally, the high signal-to-noise power spectrum of molecular material will show the growth of galaxies over the third billion years of cosmic history. Cross-correlation with existing and planned optical surveys such as the Subaru Hyper Suprime Camera (HSC) and Large Synoptic Survey Telescope (LSST) surveys will explore the gas content, metal enrichment, and evolution of individual object classes.

Molecular gas is a poorly understood but vital component of galaxy evolution. This phase of the interstellar medium (ISM) dominates the baryonic mass of early galaxies but is extremely difficult to observe. Rotational transitions of carbon monoxide (CO) are the primary probe of molecular gas. These transitions occur at integer multiples of the $J = 1 \rightarrow 0$ transition at 115 GHz; observed frequencies are shifted by the cosmological redshift. With the most sensitive arrays available it is possible to detect the molecular ISM out to redshifts as high as $z = 6.4$ [132, 133, 134, 135]. These detections demonstrate the rapid chemical enrichment of early galaxies, but they probe massive objects that are not representative of the overall population of galaxies. The CO-detected galaxies are typically the most massive and most metal rich objects of their era, significantly more luminous and massive than a Milky-Way type galaxy. ALMA and EVLA observations will transform our understanding of the molecular gas population down to Milky-Way like objects with molecular mass limits of $\sim 10^9 M_\odot$, primarily through follow-up of galaxies discovered through other surveys [136, 137]. In the study of reionization and galaxy formation, however, it is the low-mass galaxies, rather than the massive ones, that must be examined because of their very large number [138, 139].

Intensity mapping probes the distribution of lower mass galaxies through their spatial fluctuations. This signal is identifiable in the variance $(\Delta^2_{\rm CO})$ of the spatial+spectral power spectrum, as a function of the three-dimensional

wave-vector (k). The technique is a three-dimensional version of the two-dimensional techniques used to characterize the cosmic microwave background (CMB) anisotropy and is identical to the technique that has been developed for hydrogen epoch of reionization experiments [140]. The CO intensity power spectrum consists of two components: a Poisson component from the random distribution of individual galaxies and a component from the large-scale clustering of the galaxies imposed by the process of structure formation. The transition between these components occurs at $k \sim 0.3$ h Mpc^{-1}, as can be seen in the power-law break in the models (Fig. 8). In the current understanding of the reionization process, the clustered formation of galaxies sets the distribution of ionizing bubbles, and so sampling these low-k modes is of great interest.

The ngVLA can make a substantial contribution in this area. The proposed frequency range provides sensitivity to multiple transitions of CO at redshifts from $z \sim 1$ to the EoR. If designed to a maximum frequency of 115 GHz, the $2 \rightarrow 1$ transition of CO becomes available at $z > 1$, joining the $1 \rightarrow 0$ transition that is accessible, by design, at z=0. The broad frequency coverage of the array therefore permits detection of the growth of molecular gas through cross-correlation between CO transitions starting when the universe was less than half its current age. Other molecular tracers, such as formaldehyde and fainter lines, will also be accessible to ngVLA. Experiments can also be matched to individual redshift windows from deep optical spectroscopic surveys, such as those that will be carried out by Subaru, HETDEX and DESI.

The primary technical challenge for ngVLA is to provide a wide field of view and sensitivity to the shortest baselines. Large dishes and long baselines will filter out the clustered component of the intensity mapping signal. Sensitivity to scales as large as tens of arcminutes is necessary to detect the clustered component. This may be feasible with an array of small, densely-packed dishes at wavelengths ~ 2 cm ($z \sim 6$). Total power capability for the antennas would also provide the ability to mosaic large-scales and recover the clustered component.

4.3 Astrometry

Most cosmological observables, such as redshift, distance, or flux, are functions of time: given enough time or enough precision, these quantities will be seen to drift due to the Hubble expansion and the expansion's acceleration. The rate for real-time cosmological changes is of order $H_0 \sim 10^{-10}$ yr^{-1}, so the necessary precision in photometry or distance determinations does not
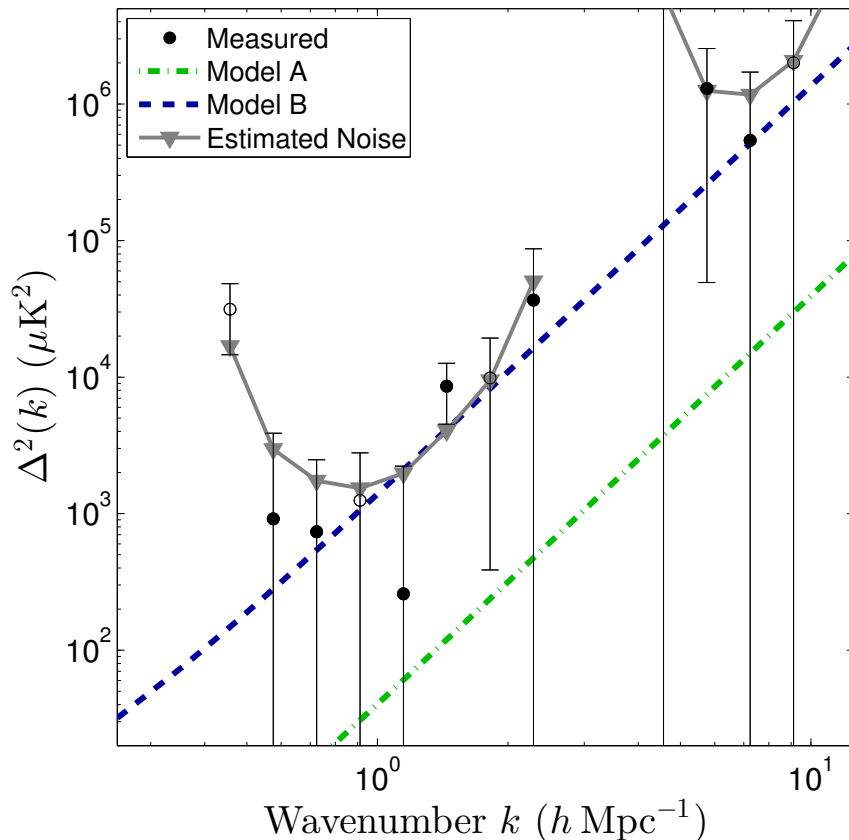
Figure 8: Power spectrum of CO intensity from $z = 2.3$ to 3.3. We show two different models (A and B) for the signal strength based on observed and theoretical star-formation estimates [141]. Sunyaev-Zel'dovich Array results from Keating et al. (2015) are shown [142].

exist (although it might be possible in the coming decades to measure the secular redshift drift [143]). When expressed as an angular motion, however, $H_0 \approx 15 \, \mu$as yr^{-1}, which is in the realm of possibility for current and future telescopes [144].

Correlated proper motions of AGN or quasars serving as test masses can reveal new "real-time" cosmological effects. Most extragalactic radio sources show significant intrinsic proper motion at VLBI resolution, which frustrates proper motion studies of individual objects. Large-scale correlated proper motions, however, are independent of internal processes and provide

detectable signals at the few-μas level, as first demonstrated with the direct detection of the secular aberration drift caused by the Solar acceleration about the Galactic Center [145].

A proper motion power spectrum can be used to characterize a vector field on the sky. Like the cosmic microwave background (CMB) fluctuations, which form a scalar power pattern on a sphere and can be decomposed into spherical harmonic amplitudes for each degree ℓ, the proper motion power spectrum can be characterized using *vector* spherical harmonics (VSH), which are the gradient and curl of the scalar spherical harmonics. The curl-free VSH resemble electric fields (E-modes, or spheroidal modes), and the divergenceless VSH resemble magnetic fields (B-modes, or toroidal modes) [146].

An ngVLA with VLBA baselines performing astrometric monitoring of 10,000 objects with 10 μas yr^{-1} astrometry per object would enable the global detection of 0.1 μas yr^{-1} correlated signals at 5σ significance, which is $\sim$0.7% of H_0. This proper motion sensitivity would provide the opportunity to detect numerous observer-induced and cosmological effects:

• The solar motion with respect to the CMB is 80 AU yr^{-1}, inducing a distance-dependent E-mode dipole with amplitude $D^{-1}(\mathrm{Mpc}) \times 80$ μas yr^{-1}. It may thus be possible to obtain individual parallax distances to galaxies out to about 8 Mpc (but peculiar motions complicate this prospect).

• Anisotropic Hubble expansion would in its simplest form appear as an E-mode quadrupole [147], and an expansion vorticity would manifest as a B-mode quadrupole. The ngVLA could constrain the isotropy of expansion to of order 0.1% of H_0.

• Very long-period gravitational waves will deflect light from distant objects in a quadrupolar (and higher order) E- and B-mode pattern on the sky [148]. The sensitivity of astrometry to gravitational waves spans frequencies from $\sim$1 yr^{-1} to H_0 (10 orders of magnitude; 10^{-18}–10^{-8} Hz), and the proposed ngVLA astrometric program could be competitive with pulsar timing (but probes a different and much larger frequency regime).

• At higher ℓ, the real-time growth and recession of large scale structure will manifest in E-modes [144]. Astrometric close pairs embedded in the same large scale structure will show a convergent proper motion distinct from randomly selected astrometric pairs of test masses and can in principle measure H_0.

• At $\ell \sim 40$, the baryon acoustic oscillation (BAO; [149]) scale, the real-time evolution of the BAO will show a convergent (E-mode) signal. At $z = 0.5$, $\theta_{BAO} = 4.5°$, and $d\theta_{BAO}/dt_0 = -1.2$ μas yr^{-1}. The real-time evolution of the BAO measures the ratio $H_0/D_A(z)$ (to first order).

Several of these real-time effects have not yet been developed theoretically, so the magnitudes of the anticipated signals are not well-constrained. The theory will be addressed prior to the full Gaia data release and should be mature by 2017.

5 Technical Requirements for Key Science

5.1 Galactic Center Pulsars

Technical requirements for the Galactic Center pulsar detection and timing are:

- Frequency coverage in 10 – 30 GHz range;

- Ability to produce a phased array beam with a substantial fraction of the collecting area. This beam is most readily achieved through a compact array configuration. For detection, the beam should have a size ~ 0.5 arcsec with a large fraction of the collecting area at 10 GHz, corresponding to $\sim 50\%$ of the collecting area within 6 km. This can be mitigated to some degree by tiled searching or multi-beam searching. For reference, the S2 star has a semi-major axis of 0.12 arcsec. For timing, the beam can be more compact. It is possible to achieve the necessary beam for timing with an extended array and fast, real-time phasing solutions.

- The phased array beam should have a time resolution of 100 microseconds and total bandwidth of 10 GHz.

5.2 Explosive Transients including EM GW Sources

Technical requirements for transient science are:

- Broad frequency coverage for SED characterization;

- Sub-arcsecond beams at all frequencies for source identification and localization;

- Survey speed sufficient to image 100 deg^2 at 10 μJy rms continuum sensitivity in 12 hours at 10 GHz: This is nominally achievable with an 18-meter dish;

- Real-time, automated telescope control to respond within minutes to triggers followed by real-time analysis and delivery of data products.

5.3   Plasma Physics

While some plasma physics problems may require very high resolution or simply point source sensitivity, the problems focused on here require imaging of large objects with relatively modest spatial resolution but high surface brightness sensitivity and fidelity. This implies the following:

- High surface bright sensitivity at 1-10 arcsec resolution. Implies a compact core for the array with at least 50% of the collecting area.

- Good mosaicking over fields of up to at least 30x30 arcmin. Argues for small dishes, perhaps 12m, with stable, well-known primary beams, to allow the smallest number of pointings and good restoration of mosaicked images.

- A broad frequency range using as few separate receivers as possible between 10-100 GHz in order to increase the effective sensitivity for spectral shape measurements.

- Some way to sample spatial frequencies on scales larger than allowed by the minimum spacing in the main array. This may require a single dish.

We need good surface brightness imaging, because the critical features which can discriminate between these models are small and bright, but also embedded in larger, extended emission regions. We need high frequencies because spectra are a key test, and a good spectral sampling across a broad frequency range (at least a decade, say) is needed to measure spectra robustly.

Since the smallest current configuration of the VLA would produce ~ 1 arcsec resolution at 100 GHz, ngVLA must have a very compact configuration with enough collecting area to yield better surface brightness sensitivity than the VLA. Furthermore, the large FOVs required means that ngVLA must work well as a a mosaicking array, since the individual telescopes will have much smaller primary beams than many of the sources of interest, e.g. the Crab, A2256 and M87. This requirement also argues for smaller array elements, perhaps 12m, in order to obtain adequate pointing for a mosaic and to reduce the number of pointings needed. Furthermore some total power mode, perhaps like ALMA or using a larger single dish, to sample the largest spatial frequencies, is needed. Given the large number of astrophysically interesting sources larger than 30 arcsec, this requirement is likely to be important for many areas of research with ngVLA. For the difficult case

of A2256 assuming a compact configuration with 3X the VLA collecting area, spectral index of -0.7 and 12m antennas, the relic could be imaged in the 10-50 GHz band using a 400 pointing mosaic with typically 20:1 S/N with 3 arcsec resolution in 25 hours.

5.4   Exoplanet Space Weather

We consider requirements for two goals.

Goal: confirm detections of stellar wind around nearby planet-hosting star, using inferences based on recent papers. Requirements are:

- RMS sensitivity of 100 nJy at 10 GHz for 5 sigma detection of radio emission from ionized wind with mass loss rate of 100 times solar mass loss rate, low velocity wind, M dwarf at 10 pc.

- RMS sensitivity of 50 nJy at 10 GHz for 5 sigma detection of radio emission from ionized wind with mass loss rate of 25 times solar mass loss rate, low velocity wind, M dwarf at 5 pc.

- Instantaneous frequency coverage of 3 GHz at 10 GHz to confirm spectral index expected for optically thick/thin emission.

Goal: diagnose magnetospheric interactions of magnetized close-in planet with host star, for a star with radio luminosity a few times 10^{13} erg/s/Hz (at the faint end of current radio detections), at a distance of 10 pc. This is sufficient to encompass the distance of any likely Earth-like planets in their host star's habitable zones. Requirements are:

- Instantaneous frequency coverage of 3 GHz or greater to diagnose changing plasma conditions.

- RMS sensitivity over 5 minutes of 1 microJy (should be equivalent to 100 nJy in 10 hours) over a bandwidth of 500 MHz, sufficient to detect robustly radio emission from a stellar source 10 pc away with $L_r =$a few times 10^{13} erg/s/Hz, and determine changing flux levels at the level of 20% to a significance of several sigma, as a function of frequency and time.

- Sensitivity to detect circularly polarized emission at the level of 20% of the total intensity in a timescale of 5 minutes, in a source with a radio luminosity of a few times 10^{13} erg/s/Hz at a distance of 10 pc.

5.5 Astrometry

Here we discuss technical considerations to achieve optimal VLBI astrometry for the ngVLA. The precision of relative astrometry ("in-beam") depends on the size of the synthesized beam and the sensitivity on long baselines. For absolute position determination, the critical parameter is simply the baseline length, along with delay error. Therefore, the one stringent requirement is that at least 20% of the collecting area of the array should cover long baselines, up to ∼5000 km, in both the east-west and north-south directions. For astrometry of compact targets, e.g. masers, good uv coverage is not essential, so the long baselines could in principle be met with 5-7 large dishes, or phased groups of smaller antennas, that would supplement the main central array. The antennas should cover observing frequencies at least up to 22 GHz.

Absolute position determination further depends on the quality of the geodetic calibration (i.e. residual atmospheric and clock delays) and phase transfer from astrometric calibrators. The technical requirements here are mild. The antennas should be able to slew fairly quickly, preferably > 40 degrees per minute, and the system should allow observing at least 1 GHz continuum bandwidth.

Finally, maser astrometry requires spectral observing modes that can cover 1 GHz contiguously with at least 25 kHz spectral resolution, to adequately sample the narrow line profiles that cover wide velocity ranges.

References

[1] Carilli, C.L. 2015 *et al.*, *Next Generation VLA Memo. No. 5: Project Overview* http://library.nrao.edu/ngvla.shtml.

[2] B. P. Abbott, *et al.*, *Phys. Rev. D* **80**, 102001 (2009).

[3] F. Acernese, *et al.*, *Classical and Quantum Gravity* **26**, 085009 (2009).

[4] B. D. Metzger, E. Berger, *ApJ* **746**, 48 (2012).

[5] K. Hotokezaka, K. Kyutoku, H. Okawa, M. Shibata, K. Kiuchi, *Phys. Rev. D* **83**, 124008 (2011).

[6] E. Nakar, T. Piran, *Nat.* **478**, 82 (2011).

[7] P. B. Demorest, T. Pennucci, S. M. Ransom, M. S. E. Roberts, J. W. T. Hessels, *Nat.* **467**, 1081 (2010).

[8] J. Antoniadis, *et al.*, *Science* **340**, 448 (2013).

[9] D. M. Siegel, R. Ciolfi, L. Rezzolla, *ApJ* **785**, L6 (2014).

[10] B. D. Metzger, G. C. Bower, *MNRAS* **437**, 1821 (2014).

[11] L. P. Singer, *et al.*, *ApJ* **795**, 105 (2014).

[12] J. G. Hills, *Nat.* **254**, 295 (1975).

[13] S. Gezari, *et al.*, *ApJ* **766**, 60 (2013).

[14] E. Berger, *et al.*, *ApJ* **748**, 36 (2012).

[15] B. A. Zauderer, *et al.*, *ApJ* **767**, 152 (2013).

[16] M. J. Rees, *Nat.* **333**, 523 (1988).

[17] J. S. Bloom, D. Giannios, B. D. Metzger, *et al.*, *Science* **333**, 203 (2011).

[18] A. J. Levan, *et al.*, *Science* **333**, 199 (2011).

[19] D. N. Burrows, *et al.*, *Nat.* **476**, 421 (2011).

[20] B. A. Zauderer, *et al.*, *Nat.* **476**, 425 (2011).

[21] D. Giannios, B. D. Metzger, *MNRAS* **416**, 2102 (2011).

[22] S. B. Cenko, *et al.*, *ApJ* **753**, 77 (2012).

[23] G. R. Farrar, A. Gruzinov, *ApJ* **693**, 329 (2009).

[24] P. Mimica, D. Giannios, B. D. Metzger, M. A. Aloy, *ArXiv e-prints* (2015).

[25] G. C. Bower, B. D. Metzger, S. B. Cenko, J. M. Silverman, J. S. Bloom, *ApJ* **763**, 84 (2013).

[26] S. van Velzen, D. A. Frail, E. Körding, H. Falcke, *A&A* **552**, A5 (2013).

[27] B. D. Metzger, P. K. G. Williams, E. Berger, *ArXiv e-prints* (2015).

[28] N. Stone, A. Loeb, *ArXiv e-prints* (2011).

[29] D. Morris, M. Kramer, C. Thum, et al., *Astron. & Astrophys.* **322**, L17 (1997).

[30] O. Löhmer, A. Jessner, M. Kramer, R. Wielebinski, O. Maron, *A&A* **480**, 623 (2008).

[31] D. R. Lorimer, *et al.*, *MNRAS* **372**, 777 (2006).

[32] J. M. Cordes, J. T. W. Lazio, *Astrophys. J.* **475**, 557 (1997).

[33] R. S. Wharton, S. Chatterjee, J. M. Cordes, J. S. Deneva, T. J. W. Lazio, *ApJ* **753**, 108 (2012).

[34] D. R. Lorimer, M. Kramer, *Handbook of Pulsar Astronomy* (Cambridge University Press, 2005).

[35] N. Wex, S. Kopeikin, *Astrophys. J.* **513**, 388 (1999).

[36] M. Kramer, *et al.*, *New Astronomy Reviews* **48**, 993 (2004).

[37] K. Liu, N. Wex, M. Kramer, J. M. Cordes, T. J. W. Lazio, *ApJ* **747**, 1 (2012).

[38] M. Kramer, *et al.*, *IAU Colloq. 177: Pulsar Astronomy - 2000 and Beyond*, M. Kramer, N. Wex, R. Wielebinski, eds. (2000), vol. 202 of *Astronomical Society of the Pacific Conference Series*, p. 37.

[39] S. Johnston, *et al.*, *MNRAS* pp. L96+ (2006).

[40] J. S. Deneva, J. M. Cordes, T. J. W. Lazio, *ApJ* **702**, L177 (2009).

[41] J.-P. Macquart, N. Kanekar, D. A. Frail, S. M. Ransom, *ApJ* **715**, 939 (2010).

[42] C.-A. Faucher-Giguère, A. Loeb, *MNRAS* **415**, 3951 (2011).

[43] L. G. Spitler, *et al.*, *ApJ* **780**, L3 (2014).

[44] G. C. Bower, *et al.*, *ApJ* **780**, L2 (2014).

[45] W. J. Marciano, *Phys. Rev. Lett.* **52**, 489 (1984).

[46] T. Damour, A. M. Polyakov, *Nucl. Phys. B* **423**, 532 (1994).

[47] J.-P. Uzan, *Living Reviews in Relativity* **14**, 2 (2011).

[48] J. K. Webb, V. V. Flambaum, C. W. Churchill, M. J. Drinkwater, J. D. Barrow, *Phys. Rev. Lett.* **82**, 884 (1999).

[49] C. R. Gould, E. I. Sharapov, S. K. Lamoreaux, *Phys. Rev. C* **74**, 024607 (2006).

[50] T. Rosenband, *et al.*, *Science* **319**, 1808 (2008).

[51] P. Molaro, *et al.*, *A&A* **555**, A68 (2013).

[52] X. Calmet, H. Fritzsch, *Eur. Phys. Jour. C* **24**, 639 (2002).

[53] P. G. Langacker, G. Segré, M. J. Strassler, *Phys. Lett. B* **528**, 121 (2002).

[54] M. T. Murphy, J. K. Webb, V. V. Flambaum, *MNRAS* **345**, 609 (2003).

[55] M. T. Murphy, *et al.*, *Astrophysics, Clocks and Fundamental Constants*, S. G. Karshenboim, E. Peik, eds. (Springer-Verlag, Berlin, 2004), vol. 648 of *Lecture Notes in Physics*, p. 131.

[56] R. Srianand, H. Chand, P. Petitjean, B. Aracil, *Phys. Rev. Lett.* **99**, 239002 (2007).

[57] M. T. Murphy, J. K. Webb, V. V. Flambaum, *MNRAS* **384**, 1053 (2008).

[58] J. K. Webb, *et al.*, *Phys. Rev. Lett.* **107**, 191101 (2011).

[59] K. Griest, *et al.*, *ApJ* **708**, 158 (2010).

[60] J. B. Whitmore, M. T. Murphy, K. Griest, *ApJ* **723**, 89 (2010).

[61] H. Rahmani, *et al.*, *MNRAS* **435**, 861 (2013).

[62] R. I. Thompson, *ApL* **16**, 3 (1975).

[63] D. A. Varshalovich, S. A. Levshakov, *JETP* **58**, L237 (1993).

[64] W. Ubachs, R. Buning, K. S. E. Eikema, E. Reinhold, *J.Mol.Spec.* **241**, 155 (2007).

[65] P. Noterdaeme, C. Ledoux, P. Petitjean, R. Srianand, *A&A* **481**, 327 (2008).

[66] F. van Weerdenburg, M. T. Murphy, A. L. Malec, L. Kaper, W. Ubachs, *Phys. Rev. Lett.* **106**, 180802 (2011).

[67] J. Bagdonaite, W. Ubachs, M. T. Murphy, J. B. Whitmore, *Phys. Rev. Lett.* **114**, 071301 (2015).

[68] J. Darling, *Phys. Rev. Lett.* **91**, 011301 (2003).

[69] J. N. Chengalur, N. Kanekar, *Phys. Rev. Lett.* **91**, 241302 (2003).

[70] V. V. Flambaum, M. G. Kozlov, *Phys. Rev. Lett.* **98**, 240801 (2007).

[71] P. Jansen, L.-H. Xu, I. Kleiner, W. Ubachs, H. L. Bethlem, *Phys. Rev. Lett.* **106**, 100801 (2011).

[72] S. A. Levshakov, M. G. Kozlov, D. Reimers, *ApJ* **738**, 26 (2011).

[73] M. G. Kozlov, S. A. Levshakov, *ApJ* **726**, 65 (2011).

[74] T. Wiklind, F. Combes, *A&A* **286**, L9 (1994).

[75] T. Wiklind, F. Combes, *A&A* **299**, 382 (1995).

[76] T. Wiklind, F. Combes, *A&A* **315**, 86 (1996).

[77] T. Wiklind, F. Combes, *Nature* **379**, 139 (1996).

[78] N. Kanekar, *et al.*, *Phys. Rev. Lett.* **95**, 261301 (2005).

[79] N. Kanekar, *ApJ* **728**, L12 (2011).

[80] N. Kanekar, *et al.*, *MNRAS* **448**, L104 (2015).

[81] J. Bagdonaite, *et al.*, *Science* **339**, 46 (2013).

[82] J. Bagdonaite, *et al.*, *Phys. Rev. Lett.* **111**, 231101 (2013).

[83] N. Kanekar, A. Gupta, C. L. Carilli, J. T. Stocke, K. W. Willett, *ApJ* **782**, 56 (2014).

[84] N. Kanekar, J. N. Chengalur, T. Ghosh, *ApJ* **716**, L23 (2010).

[85] N. Kanekar, G. I. Langston, J. T. Stocke, C. L. Carilli, K. M. Menten, *ApJ* **746**, L16 (2012).

[86] J. A. King, M. T. Murphy, W. Ubachs, J. K. Webb, *MNRAS* **417**, 301 (2011).

[87] M. Wendt, P. Molaro, *A&A* **541**, A69 (2012).

[88] D. Albornoz Vásquez, *et al.*, *A&A* **562**, A88 (2014).

[89] V. V. Ilyushin, *et al.*, *Phys. Rev. A* **85**, 032505 (2012).

[90] M. G. Kozlov, *Phys. Rev. A* **84**, 042120 (2011).

[91] L. O. Drury, *Reports on Progress in Physics* **46**, 973 (1983).

[92] M. M. Romanova, R. V. E. Lovelace, *A&A* **262**, 26 (1992).

[93] S. Zenitani, M. Hoshino, *ApJ* **562**, L63 (2001).

[94] F. Guo, H. Li, W. Daughton, Y.-H. Liu, *Physical Review Letters* **113**, 155005 (2014).

[95] M. F. Bietenholz, Y. Yuan, R. Buehler, A. P. Lobanov, R. Blandford, *MNRAS* **446**, 205 (2015).

[96] R. Bühler, R. Blandford, *Reports on Progress in Physics* **77**, 066901 (2014).

[97] L. Sironi, A. Spitkovsky, *ApJ* **741**, 39 (2011).

[98] R. G. Arendt, *et al.*, *ApJ* **734**, 54 (2011).

[99] F. N. Owen, *et al.*, *ApJ* **794**, 24 (2014).

[100] L. Feretti, G. Giovannini, F. Govoni, M. Murgia, *A&A Rev.* **20**, 54 (2012).

[101] S. W. Skillman, *et al.*, *ApJ* **765**, 21 (2013).

[102] A. Stroe, J. J. Harwood, M. J. Hardcastle, H. J. A. Röttgering, *MNRAS* **445**, 1213 (2014).

[103] T. E. Clarke, T. A. Ensslin, *AJ* **131**, 2900 (2006).

[104] D. Kagan, M. Milosavljević, A. Spitkovsky, *ApJ* **774**, 41 (2013).

[105] G. Benford, *ApJ* **333**, 735 (1988).

[106] G. Paschmann, S. Haaland, R. Treumann, *Auroral Plasma Physics* (2003).

[107] H. Lesch, G. T. Birk, *A&A* **324**, 461 (1997).

[108] F. N. Owen, J. A. Eilek, N. E. Kassim, *ApJ* **543**, 611 (2000).

[109] Y. Shi, G. H. Rieke, D. C. Hines, K. D. Gordon, E. Egami, *ApJ* **655**, 781 (2007).

[110] M. Güdel, *ARA&A* **40**, 217 (2002).

[111] A. E. Wright, M. J. Barlow, *MNRAS* **170**, 41 (1975).

[112] N. Panagia, M. Felli, *A&A* **39**, 1 (1975).

[113] B. E. Wood, H.-R. Müller, G. P. Zank, J. L. Linsky, S. Redfield, *ApJ* **628**, L143 (2005).

[114] A. Vidal-Madjar, *et al.*, *Nat.* **422**, 143 (2003).

[115] A. Lecavelier des Etangs, *et al.*, *A&A* **543**, L4 (2012).

[116] M. Massi, *et al.*, *A&A* **453**, 959 (2006).

[117] I. Pillitteri, *et al.*, *ApJ* **785**, 145 (2014).

[118] C. H. Jackman, A. R. Douglass, R. B. Rood, R. D. McPeters, P. E. Meade, *J. Geophys. Res.* **95**, 7417 (1990).

[119] Planck Collaboration, *et al.*, *ArXiv e-prints* (2015).

[120] A. G. Riess, *et al.*, *ApJ* **730**, 119 (2011).

[121] W. L. Freedman, *et al.*, *ApJ* **758**, 24 (2012).

[122] J. R. Herrnstein, *et al.*, *Nat.* **400**, 539 (1999).

[123] C. Y. Kuo, *et al.*, *ApJ* **727**, 20 (2011).

[124] J. E. Greene, *et al.*, *ApJ* **721**, 26 (2010).

[125] M. J. Reid, *et al.*, *ApJ* **767**, 154 (2013).

[126] C. Y. Kuo, *et al.*, *ApJ* **767**, 155 (2013).

[127] C. Y. Kuo, *et al.*, *ApJ* **800**, 26 (2015).

[128] J. D. Bowman, A. E. E. Rogers, *Nat.* **468**, 796 (2010).

[129] S. Yatawatta, *et al.*, *A&A* **550**, A136 (2013).

[130] A. R. Parsons, *et al.*, *ApJ* **788**, 106 (2014).

[131] A. Lidz, *et al.*, *ApJ* **741**, 70 (2011).

[132] P. M. Solomon, P. A. Vanden Bout, *ARA&A* **43**, 677 (2005).

[133] R. Wang, *et al.*, *AJ* **142**, 101 (2011).

[134] D. A. Riechers, *et al.*, *Nat.* **496**, 329 (2013).

[135] J. D. Vieira, *et al.*, *Nat.* **495**, 344 (2013).

[136] R. J. Ivison, *et al.*, *MNRAS* **412**, 1913 (2011).

[137] R. Wang, *et al.*, *IAU Symposium*, T. Wong, J. Ott, eds. (2013), vol. 292 of *IAU Symposium*, pp. 184–187.

[138] R. J. Bouwens, *et al.*, *ApJ* **752**, L5 (2012).

[139] B. E. Robertson, *et al.*, *ApJ* **768**, 71 (2013).

[140] M. F. Morales, J. Hewitt, *ApJ* **615**, 7 (2004).

[141] A. R. Pullen, T.-C. Chang, O. Doré, A. Lidz, *ApJ* **768**, 15 (2013).

[142] G. K. Keating, G. C. Bower, D. P. Marrone, C. E. Heiles, D. R. De-Boer, *American Astronomical Society Meeting Abstracts* (2015), vol. 225 of *American Astronomical Society Meeting Abstracts*, p. 427.05.

[143] J. Darling, *ApJ* **761**, L26 (2012).

[144] J. Darling, *ApJ* **777**, L21 (2013).

[145] O. Titov, S. B. Lambert, A.-M. Gontier, *A&A* **529**, A91 (2011).

[146] F. Mignard, S. Klioner, *A&A* **547**, A59 (2012).

[147] J. Darling, *MNRAS* **442**, L66 (2014).

[148] L. G. Book, É. É. Flanagan, *Phys. Rev. D* **83**, 024024 (2011).

[149] D. J. Eisenstein, *et al.*, *ApJ* **633**, 560 (2005).